

Abstract

In the fall of 2013, the Vaisala RS41-SG (4th generation) radiosonde was introduced as a replacement for the RS92-SGP radiosonde with improvements in measurement accuracy of profiles of atmospheric temperature, humidity and pressure. In order to help characterize these improvements, an intercomparison campaign was undertaken at the US Department of Energy's Atmospheric Radiation Measurement (ARM) Facility site in north Central Oklahoma USA. During 3–8 June 2014, a total of 20 twin-radiosonde flights were performed in a variety of atmospheric conditions representing typical mid-latitude continental summertime conditions. The results suggest that the RS92 and RS41 measurements generally agree within manufacturer specified tolerances with notable exceptions when exiting liquid cloud layers where the “wet bulbing” effect is mitigated in the RS41 observations. The RS41 measurements also appear to show a smaller impact from solar heating. These results suggest that the RS41 does provide important improvements, particularly in cloudy conditions, but under most observational conditions the RS41 and RS92 measurements agree within the manufacturer specified limits and so a switch to RS41 radiosondes will have little impact on long-term observational records.

1 Introduction

Since the 1930s measurements of tropospheric temperature, pressure, water vapor and winds have been made by radiosondes attached to balloons. These measurements provide critical input to weather forecasting and climate models, quantification of atmospheric thermodynamic stability, input to remote sensing retrievals and important constraints for atmospheric process studies. The long history of radiosonde observations includes many changes in instrumentation, practices, processing and other issues (e.g., Elliot and Gaffen, 1991, 1993; Elliot et al., 1998; Wang et al., 2003; Rowe et al., 2008; McCarthy et al., 2009; Milosevich et al., 2009; Zhao et al., 2012).

AMTD

8, 11323–11368, 2015

Comparison of Vaisala radiosondes RS41 and RS92

M. P. Jensen et al.

Title Page

Abstract

Introduction

Conclusions

References

Tables

Figures



Back

Close

Full Screen / Esc

Printer-friendly Version

Interactive Discussion



Comparison of Vaisala radiosondes RS41 and RS92

M. P. Jensen et al.

Title Page

Abstract

Introduction

Conclusions

References

Tables

Figures



Back

Close

Full Screen / Esc

Printer-friendly Version

Interactive Discussion



The US Department of Energy's Atmospheric Radiation Measurement (ARM) Climate Research Facility (Mather and Voyles, 2013; Ackerman and Stokes, 2003; Stokes and Schwartz, 1994; <http://www.arm.gov>) operates three fixed field sites (Southern Great Plains (SGP) Oklahoma, USA; North Slope, Alaska, USA; and Eastern North Atlantic, Azores, Portugal) and three mobile field sites to study the effects of aerosols, precipitation, surface fluxes and clouds on global climate. One important component of the measurements at each of these sites is the routine launching of radiosondes 2–4 times per day resulting in more than 5000 launches per year. During this period the ARM program has used Vaisala radiosondes as part of regular operations and intensive operational periods (e.g., Ghan et al., 2000; Xu et al., 2002; Xie et al., 2005; Miller et al., 2007; Jensen et al., 2015a, b). The RS92-SGP radiosonde is the current standard at all of the ARM sites and has been in use since 2005. The observations from these soundings have been used for many scientific applications including the derivation of large-scale forcing datasets for modeling studies (e.g., Zhang and Lin, 1997; Zhang et al., 2001; Xie et al., 2010, 2015), constraints on cloud remote sensing retrievals (e.g., Zhao et al., 2012; Huang et al., 2012; Dunn et al., 2011) and quantification of atmospheric thermodynamic structure (e.g., Sawyer and Li, 2013; McFarlane et al., 2013).

The Vaisala RS41-SG (4th generation) radiosonde was first developed to replace the RS92-SGP and was introduced in the fall of 2013 with new technological solution aimed at delivering improvements in measurement accuracy of profiles of atmospheric temperature, humidity and pressure. In order to characterize the improvements and differences of the RS41-SG radosonde compared to the RS92-SGP, a number of intercomparison campaigns have been undertaken in varying environments, including midlatitude test campaigns at Libus, Prague Czech Republic (Motl, 2014), in August 2013 and by the UK Met Office at Camborne, UK (Edwards et al., 2014) in November 2013. Higher latitude testing has been done in Finland (Vantaa and Sodankyla) and tropical conditions were sampled in Penang, Malaysia (Jauhiainen et al., 2014). This manuscript will describe the results of an intercomparison study of the new RS41-SG

Comparison of Vaisala radiosondes RS41 and RS92

M. P. Jensen et al.

Title Page

Abstract

Introduction

Conclusions

References

Tables

Figures



Back

Close

Full Screen / Esc

Printer-friendly Version

Interactive Discussion



that there is also a model RS41-SGP radiosonde with a pressure sensor similar to the RS92) while the RS92 uses a silicon, capacitive sensor. The GPS-derived values of the RS41 have improved resolution and improved accuracy at pressures lower than 100 mb compared to the RS92 sensor measured pressure (Table 4, Vaisala, 2014).

Both the RS41 and RS92 use GPS to derive wind speed and direction with similar measurement performance (velocity uncertainty = 0.15 ms^{-1} , direction uncertainty = 2 deg, Vaisala, 2014).

In general, the two radiosonde models apply similar types of corrections for the edited pressure, temperature and humidity sounding data. However, there are a couple of significant differences between the corrections worth mentioning. In the ground check phase, no ground check correction is applied for the RS41 temperature measurement. A functionality check and a comparison of readings with the temperature sensor of the humidity sensor chip are performed instead. Another major difference is related to the approach on how the humidity measurements take into account the effect of solar radiation. In the case of the RS92, the increment in humidity sensor temperature is estimated taking into account the solar radiation intensity and the related physics, and the humidity measurement result is corrected accordingly. On the contrary, the RS41 humidity sensor incorporates an on-chip temperature sensor, and, thus, the temperature of the humidity sensor is continuously measured and taken into account in the relative humidity calculations. In other words, no solar radiation correction is needed nor applied for the RS41 humidity measurement.

A notable difference in the two sounding systems is that the launch procedure for the RS41 radiosonde is much simpler than that for the RS92. In particular, the RS41 is powered with integrated batteries removing the need to open the body and connect the battery as in the RS92. The RS41 also has status LED indicators which indicate launch readiness as the radiosonde goes through the ground check procedure and self-diagnostics prior to launch. Also, the RS41 ground check device enables an accurate zero humidity check without the use of a desiccant, as in the GC25 ground check device used with the RS92. This change removes the need for maintenance of the desiccant,

Comparison of Vaisala radiosondes RS41 and RS92

M. P. Jensen et al.

Title Page

Abstract

Introduction

Conclusions

References

Tables

Figures



Back

Close

Full Screen / Esc

Printer-friendly Version

Interactive Discussion



From 3–7 June 2014, a series of weather balloon flights were performed at the ARM SGP Central Facility (36.695° latitude, –97.485° longitude) with the goal of evaluating the relative performance of the RS92/MW31 and RS41/MW41 radiosondes/systems. The June time period at SGP represented a summertime mid-latitude convective environment during which the extensive remote sensing observations at the SGP site were used to further quantify the environment during the intercomparison. Over the course of five days a total of 20 balloon flights were completed with efforts to sample the entire diurnal cycle and a variety of cloud conditions (avoiding heavy precipitation, which could result in launch failures).

Table 5 summarizes the basic characteristics of the 20 radiosonde flights at the ARM SGP site. Efforts were made to sample the daytime diurnal cycle and also to include several nighttime flights where heating by solar radiation would not be an issue. All 20 flights were considered successful with sampling through the atmosphere to a height of at least 28 km for 19 of the 20 soundings (the final flight terminated at a height just below 26 km). Over the course of five days, a range of different meteorological conditions was observed. Figure 5 shows the time series of (a) precipitable water vapor as retrieved from a two-channel microwave radiometer (Turner et al., 2007), (b) surface dry-bulb temperature and relative humidity, (c) hemispheric sky cover as observed from a total sky imager (Long et al., 2001). Table 6 shows the numerical values of these quantities at the launch time for each sounding. A variety of conditions were sampled including six nighttime soundings, surface temperatures ranging from 20.4 to 33.1 °C, surface relative humidity ranging from 46–96%, precipitable water vapor ranging from 2.55 to 4.77 cm and hemispheric sky cover ranging from 2 to 100%. Figure 6 shows hourly profiles of cloud frequency of occurrence derived from the Active Remote Sensing of CLOUDs value-added data product (Clothiaux et al., 2000; Kollias et al., 2007) that uses a combination of Ka-band Zenith Pointing Radar (KAZR), Micropulse Lidar (MPL) and ceilometer observations to produce a best estimate of cloud occurrence. Occurrence statistics are determined over a 1 h time window and a 30 m height window. Vertical black lines represent the times of dual-radiosonde launches.

Launches occurred for a variety of cloud conditions including single- and multi-layer low and high-level clouds.

4 Results

Figure 7 shows a typical example, from the 3 June 2014 at 17:46 LT balloon flight #3, of the observations collected during a weather balloon flight. This profile shows a temperature inversion with a base near 775 mb and a very dry troposphere above. The convective available potential energy (CAPE) exceeds 2200 J kg^{-1} while the convective inhibition (CIN) is approximately -315 J kg^{-1} . Both CAPE and CIN are calculated by characterizing the surface parcel as the maximum virtual temperature in the lowest 1 km and integrating the buoyancy at all observed sounding levels (Jensen et al., 2015b). The RS41 and RS92 radiosondes showed very similar results for all measurement quantities where the differences between the radiosonde types are much smaller than the variability in a single profile.

For the purposes of calculating quantitative differences between the soundings, we interpolate the RS92 profiles to the same time-step as the RS41 and then, using the RS41 GPS-derived heights, onto a common vertical grid with 10 m vertical resolution. Figure 8 shows a summary of the vertical profiles of differences in barometric pressure, dry-bulb temperature, relative humidity, zonal wind speed and meridional wind speed between the RS92 and RS41 measurements. For each quantity we plot the median, 25th/75th percentile and 10th/90th percentile difference over all 20 soundings for each height on the interpolated grid. The RS41 calculated pressure is greater than that observed by the RS92 at all heights (Fig. 8a) for about half (52 %) of the observations. This results in a maximum (minimum) in the median difference [RS92 – RS41] of 0.20 (–0.56) hPa at a height of 5.63 (0.61) km. These differences are well within the defined accuracy of the radiosonde systems (see Table 4) and are consistent with the results of Motl (2014) who report a maximum difference of 0.3 hPa decreasing to zero at higher levels. For dry bulb temperature (Fig. 8b), the median difference as a func-

Comparison of Vaisala radiosondes RS41 and RS92

M. P. Jensen et al.

Title Page

Abstract

Introduction

Conclusions

References

Tables

Figures



Back

Close

Full Screen / Esc

Printer-friendly Version

Interactive Discussion



Comparison of Vaisala radiosondes RS41 and RS92

M. P. Jensen et al.

Title Page

Abstract

Introduction

Conclusions

References

Tables

Figures



Back

Close

Full Screen / Esc

Printer-friendly Version

Interactive Discussion



tion of height does not exceed $0.13\text{ }^{\circ}\text{C}$ below 28 km. This is consistent with the results of Jauhiainen et al. (2014) who showed mean differences did not exceed $0.2\text{ }^{\circ}\text{C}$ during their sounding intercomparison in the Czech Republic. When considering all of the temperature observations at all heights the mean difference is $-0.014\text{ }^{\circ}\text{C}$. The absolute value of the difference exceeds $0.5\text{ }^{\circ}\text{C}$ (the combined uncertainty in RS92 temperature measurements, see Table 2) for only 0.59% of the observations. The large negative temperature difference (RS41 temperature greater than RS92 temperature) in the 10th percentile curve at 2.2 km comes from flights number 9 and 10. Sixty-seven percent of the RS41 observations below 28 km indicate a larger relative humidity compared to the RS92 (Fig. 8c), with over 90% of the observations agreeing to within 2% RH. The peak in the median differences occurs near 10 km. At 2.2 km there is again noticeable feature where the RS41 measurement is significantly moister (8.2%) than the RS92 that comes from soundings 9 and 10.

Figures 9 and 10 are used to examine the details of the differences during these two flights. For both soundings, the RS92 shows a cooler temperature (Fig. 9b and d) and larger relative humidity (Fig. 9a and c) compared to the RS41 at heights from approximately 2.1–2.3 km. Figure 10 indicates that there is a liquid cloud layer with a cloud top height near 1.8 km most noticeable after 15:00 UTC but also present during intermittent precipitation prior to that. The large temperature (and relative humidity) differences are occurring shortly after passing through the cloud layer into a dry atmospheric layer that begins at approximately 2.1 km. The additional cooling of the RS92 is likely due to the “wet-bulbing” effect whereby the RS92 sensor became wet as it passed through the cloud layer and then is subject to evaporative cooling after entering the dry layer above cloud. Both the RS92 and RS41 radiosondes use a hydrophobic coating on the temperature sensor in order to reduce the “wet-bulbing” effect without impacting the temperature measurements. However, consistent with the results of Edwards et al. (2014), the RS41 is less prone to “wet-bulbing” effects compared to the RS92 during our intercomparison.

Comparison of Vaisala radiosondes RS41 and RS92

M. P. Jensen et al.

Title Page

Abstract

Introduction

Conclusions

References

Tables

Figures



Back

Close

Full Screen / Esc

Printer-friendly Version

Interactive Discussion



Figure 8d and e show the observed differences for the zonal and meridional wind profiles. The maximum (absolute value) difference below 28 km in the median zonal (meridional) wind speed is 0.086 (0.119) ms^{-1} at a height of 14.81 (1.22) km. 99.7 (99.5) % of the zonal (meridional) wind speeds agree within 0.5ms^{-1} . This is consistent with the results of Motl (2014) who found differences in the wind velocities to be less than 0.1ms^{-1} for all levels. Edwards et al. (2014), using averages over 1 km deep layers, found differences in the zonal (meridional) wind speed to generally be around $+0.01$ (-0.01 to -0.03). These small differences are not unexpected as the RS92 and RS41 use the same technique to derive winds from GPS location observations.

The overall differences in pressure, dry bulb temperature, relative humidity and wind speeds observed during this study are consistent with those quantified by Motl (2014), Edwards et al. (2013) and Jauhainen et al. (2014).

The relative peaks in the temperature and relative humidity differences near a height of 10 km are likely related to a combination of increased radiative heating of sensors due to contributions from cloud albedo, “wet-bulbing” effects and sensor response time in regions of strong gradients as the sondes traverse cloud layers. Figure 11 summarizes the frequency of occurrence of cloud layers during the radiosonde flights. Using the ARSCL data product, the number of soundings for which the cloud occurrence exceeds 25 % for the hour of the sonde launch, for each 30 m layer, is shown. This distribution shows a sharp peak near 2 km and a broader peak around 8–10 km. This peak in cloud occurrence at 8–10 km is coincident with broad maximums in the distributions of pressure, temperature and relative humidity differences between the sonde types (Fig. 8a–c) suggesting that sonde measurements in and around clouds represent the largest differences between the two sonde types.

In order to further quantify the impact of clouds on the observed differences between the RS41 and RS92 radiosondes, we categorize the sounding flights by the observed cloud conditions (cc#) based on ARSCL derived profiles of cloud frequency of occurrence during the hour of the sounding launch. We define eight broad cloud categories for the sounding times, summarized in Table 7. The differences in pressure between

Comparison of Vaisala radiosondes RS41 and RS92

M. P. Jensen et al.

Title Page

Abstract

Introduction

Conclusions

References

Tables

Figures



Back

Close

Full Screen / Esc

Printer-friendly Version

Interactive Discussion



humidity are generally less than 1 % (94 % of heights) with the RH_{RS41} almost always greater than the RH_{RS92} showing slightly smaller differences during the nighttime below approximately 5 km and above approximately 12 km (with RH_{RS92} sometimes exceeding RH_{RS41}). It must be noted that although we show smaller differences between the sounding observations at nighttime compared to daytime, that clouds, notably differences in their occurrences for daytime and nighttime observations could be driving the observed differences. Figure 14 shows profiles of the cloud frequency of occurrence compiled over the hour in which a sounding launch occurred for daytime, nighttime and all launches. Both daytime and nighttime profiles include a low-level peak near 2 km. Daytime cases have a broad double peak in the mid- to upper troposphere (5–11 km), similar to cloud category 4, while the nighttime cases have a second peak above 12 km, similar to cloud category 2. While the cloud influences on the radiosonde observations will certainly contribute to the differences shown in Fig. 13, comparisons of individual profiles of daytime and nighttime soundings under similar cloud conditions (not shown) indicate that the day/night differences are persistent.

In order to investigate other environmental factors that may impact the radiosonde observations, we partition the comparison statistics by independent measurements of the precipitable water vapor (PWV) retrieved from microwave radiometer measurements, sky cover (SC) measured by a total sky imager, and surface RH and surface temperature from in situ surface meteorology sensors. For these comparisons we partition the radiosonde observations based on the median (adjusted for significant digits) of the independent measurements at the 20 launch times: 3.6 cm for PWV, 40 % for sky cover, 65.2 % for surface RH and 26.5 °C for surface temperature. Figure 15 shows this comparison for median profiles of dry bulb temperature differences. The median profiles of dry bulb temperature differences show little sensitivity to the environmental PWV (Fig. 15a). The profiles for the lowest and highest PWVs match very closely. For 99 % of the heights, the median temperature differences for the highest and lowest PWV agree to within 0.02 °C. When partitioning the difference profiles by sky cover observations, it should be noted that the TSI does not report sky cover at night, so

Comparison of Vaisala radiosondes RS41 and RS92

M. P. Jensen et al.

Title Page

Abstract

Introduction

Conclusions

References

Tables

Figures



Back

Close

Full Screen / Esc

Printer-friendly Version

Interactive Discussion



a temperature of -45°C where $\text{RH}_{92} > \text{RH}_{41}$ by 0.1 %. Finally the difference increases to lower temperatures ($\text{RH}_{41} > \text{RH}_{92}$). In the other three RH ranges (20–40, 40–60, 60–80 %), there is a consistent trend of the difference increasing with temperature to -40°C and then decreasing to colder temperatures. This difference has a maximum of nearly 2.5 % RH at -35°C for RH in the range of 40–60 %. These differences are similar in magnitude to those observed by Edwards et al. (2014).

A benefit of performing this intercomparison at the ARM SGP site is the ability to leverage the other measurements that are available. We have already used these observations to classify the atmospheric state and cloud conditions for partitioning statistics in the radiosonde comparisons. Here we use retrieved estimates of PWV from a microwave radiometer as an independent standard to compare the radiosonde observations.

Figure 19 shows a comparison of PWV for the RS92 (red), RS41 (green) and microwave radiometer (blue) for each radiosonde flight. Error bars on the MWR observations represent the range of observed PWV during the first half hour (since the bulk of the water vapor will be in the lower troposphere) of each balloon flight. Several previous comparisons between PWV calculated from radiosonde, MWR and GPS observations have shown general agreement within 1–2 mm (Emardson et al., 2000; Niell et al., 2001; Li et al., 2003; Garcia-Lorenz et al., 2009). For all but one flight (#15) the PWV calculated from both soundings is greater than the mean PWV over the first half hour of the flight calculated from the MWR retrieval. This is consistent with the results of Jensen et al. (2015b) and likely the impact of clouds, which are not accounted for in the applied corrections. Previous comparison studies done in much drier conditions (Survo et al., 2015) showed slightly lower PWV measurements from the MWR compared to both the RS41 and RS92 radiosondes. For 14(11) of the flights the PWV calculated from the RS41(RS92) is greater than the largest PWV retrieved from the MWR over the first half hour of the flight. The PWV from the RS41 exceeds that from the RS92 for 11 of the flights with the differences ($\text{PWV}_{\text{RS92}} - \text{PWV}_{\text{RS41}}$) ranging from -0.74 to $+0.49$ mm. This agreement is well within the RS92 PWV uncertainty of ± 2 mm (Yu

et al., 2014) based on Global Climate Observing System (GCOS) Reference Upper-Air Network (GRUAN) RH uncertainly estimates.

5 Summary and conclusions

The Vaisala RS41 radiosonde was developed to replace the RS92 radiosonde, aimed at improving the accuracy of measurements of profiles of atmospheric temperature, humidity and pressure. In order to help characterize these improvements, an intercomparison campaign was undertaken at the ARM SGP site in North Central Oklahoma USA in June 2014. During this campaign, a total of 20 dual radiosonde flights were performed in a variety of atmospheric conditions representing typical midlatitude continental summertime conditions. The results suggest that the RS92 and RS41 measurements generally agree within manufacturer specified tolerances with notable exceptions when exiting liquid cloud layers where the “wet bulbing” effect is mitigated in the RS41 observations. The RS41 also appears to show a smaller impact from solar heating. These results suggest that the RS41 does provide important improvements, particularly in cloudy conditions, but under most observational conditions, the RS41 and RS92 measurements agree to within the manufacturer specified limits and so a switch to RS41 radiosondes will have little impact on long-term observational records.

The sounding dataset collected during this intercomparison (Jensen and Toto, 2015) is available from the ARM PI data archive (<http://www.arm.gov/data/pi>). All other ARM datasets (those used in the analysis and others) are available from the ARM archive (www.archive.arm.gov) and can be found using the ARM data discovery tool.

Acknowledgements. Participation by M. Jensen, D. Holdridge, T. Toto and K. Johnson was funded by the DOE ARM Program. S. Baxter was supported by the DOE, Office of Science, and Office of Workforce Development for Teachers and Scientists (WDTS) under the Science Undergraduate Laboratory Internship (SULI) Program. Data were obtained from the ARM program sponsored by the US Department of Energy, Office of Science, Office of Biological and Environmental Research, Climate and Environmental Sciences Division. The DOE ARM Pro-

Comparison of Vaisala radiosondes RS41 and RS92

M. P. Jensen et al.

Title Page

Abstract

Introduction

Conclusions

References

Tables

Figures



Back

Close

Full Screen / Esc

Printer-friendly Version

Interactive Discussion



gram provided RS92 radiosondes, balloons, unwinders and parachutes. We would also like to acknowledge the technical support from ARM SGP Central Facility operations staff, logistical support from the BNL Office of Educational Programs, and support in campaign arrangements from Vaisala.

5 References

- Ackerman, T. P. and Stokes, G. M.: The atmospheric radiation measurement program, *Phys. Today*, 56, 38–45, 2003.
- Clothiaux, E. E., Ackerman, T. P., Mace, G. G., Moran, K. P., Marchand, R. T., Miller, M. A., and Martner, B. E.: Objective determination of cloud heights and radar reflectivities using a combination of active remote sensors at the ARM CART sites, *J. Appl. Meteorol.*, 39, 645–665, 2000.
- Dunn, M., Johnson, K. L., and Jensen, M. P.: The Microbase Value-Added Product: A Baseline Retrieval of Cloud Microphysical Properties, US Department of Energy, Office of Science, Office of Biological and Environmental Research, Gaithersburg, MD, USA, DOE/SC-ARM/TR-095, 2011.
- Edwards, Anderson, D. G., Oakley, T., and Gault, P.: Met Office Intercomparison of Vaisala RS92 and RS41 Radiosondes, Met Office, Exeter, UK, Met Office Report, 89 pp., 2013.
- Elliott, W. P. and Gaffen, D. J.: On the utility of radiosonde humidity archives for climate studies, *B. Am. Meteorol. Soc.*, 72, 1507–1520, 1991.
- Elliot, W. P., Ross, R. J., and Schwartz, B.: Effects on climate records of changes in national weather service humidity processing procedures, *J. Climate*, 11, 2424–2436, 1998.
- Emardson, T. R., Johansson, J., and Elgered, G.: The systematics behavior of water vapor estimates using four years's of GPS observations, *IEEE T. Geosci. Remote*, 38, 324–329, 2000.
- Gaffen, D. J.: Historical changes in radiosonde instruments and practices, World Meteorological Organization, Geneva, Switzerland, WMO Instruments and Observing Methods Rep., 50, 123 pp., 1993.
- Garcia-Lorenzo, B., Castro-Almazan, J. A., Eff-Darwich, A., Munoz-Tunon, C., Pinilla-Alonso, N., Rodrigues-Espinosa, J. M., and Romero, I.: Precipitable water vapour content

Comparison of Vaisala radiosondes RS41 and RS92

M. P. Jensen et al.

Title Page

Abstract

Introduction

Conclusions

References

Tables

Figures



Back

Close

Full Screen / Esc

Printer-friendly Version

Interactive Discussion



Comparison of Vaisala radiosondes RS41 and RS92

M. P. Jensen et al.

Title Page

Abstract

Introduction

Conclusions

References

Tables

Figures



Back

Close

Full Screen / Esc

Printer-friendly Version

Interactive Discussion



- above the Roque de los Muchachos observatory from GPS estimations, in: Proc. SPIE 7475, Remote Sensing of Clouds and the Atmosphere XIV, 74751H, doi:10.1117/12.830235, 2009.
- Ghan, S. J., Randall, D. A., Xu, K.-M., Cederwall, R., Cripe, D., Hack, J., Icobellis, S., Klein, S., Krueger, S. K., Lohmann, U., Pedretti, J., Robock, A., Rotsayn, L., Somerville, R., Stechikov, G., Sud, Y., Walker, G., Xie, S. C., Yio, J., and Zhang, M. H.: An intercomparison of single column model simulations of summertime midlatitude continental convection, *J. Geophys. Res.*, 105, 2091–2124, 2000.
- Huang, D., Zhao, C., Dunn, M., Dong, X., Mace, G. G., Jensen, M. P., Xie, S., and Liu, Y.: An intercomparison of radar-based liquid cloud microphysics retrievals and implications for model evaluation studies, *Atmos. Meas. Tech.*, 5, 1409–1424, doi:10.5194/amt-5-1409-2012, 2012.
- Jauhainen, H., Survo, P., Lehtinen, R., and Lentonen, J.: Radiosonde RS41 and RS92 key differences and comparison test results in different locations and climates, TECO-2014, WMO Technical Conference on Meteorological and Environmental Instruments and Methods of Observations, Saint Petersburg, Russian Federation, 7–9 July 2014, P3(16), 2014.
- Jensen, M. P.: Comparison of Vaisala RS92 and RS41 Radiosonde at the ARM Southern Great Plains Site, *Vaisala News*, 194, 4–5, 2015.
- Jensen, M. P. and Toto, T.: Soundings from SGP, June 2014 Sounding Intercomparison, 3 June – 8 June 2014, 36°36′18.0″ N, 97°29′6.0″ W: Southern Great Plains Central Facility Atmospheric Radiation Measurement (ARM) Climate Research Facility Data Archive, Oak Ridge, Tennessee, USA, doi:10.5439/1171962, 2015.
- Jensen, M. P., Petersen, W. A., Bansemer, A., Bharadwaj, N., Carey, L. D., Cecil, D. J., Collis, S. M., Del Genio, A. D., Dolan, B., Gerlach, J., Giangrande, S. E., Heymsfield, A., Heymsfield, G. M., Kollias, P., Lang, T. J., Nesbitt, S. W., Neumann, A., Poellot, M. R., Rutledge, S. A., Schwaller, M. R., Tokay, A., Williams, C. R., Wolff, D. B., Xie, S., and Zipser, E. J.: The Midlatitude Continental Convective Clouds Experiment (MC3E), *B. Am. Meteorol. Soc.*, accepted, 2015a.
- Jensen, M. P., Toto, T., Troyan, D., Ciesielski, P. E., Holdridge, D., Kyrouac, J., Schatz, J., Zhang, Y., and Xie, S.: The Midlatitude Continental Convective Clouds Experiment (MC3E) sounding network: operations, processing and analysis, *Atmos. Meas. Tech.*, 8, 421–434, doi:10.5194/amt-8-421-2015, 2015b.
- Kollias, P., Miller, M. A., Luke, E. P., Johnson, K. L., Clothiaux, E. E., Moran, K. P., Widener, K. B., and Albrecht, B. A.: The atmospheric radiation measurement program cloud profiling radars:

Comparison of Vaisala radiosondes RS41 and RS92

M. P. Jensen et al.

Title Page

Abstract

Introduction

Conclusions

References

Tables

Figures



Back

Close

Full Screen / Esc

Printer-friendly Version

Interactive Discussion



Xu, K.-M., Cederwall, R. T., and Xie, S.: An intercomparison of cloud-resolving models with the ARM summer 1997 IOP data, *Q. J. Roy. Meteor. Soc.*, 128, 593–624, 2002.

Yu, H., Ciesielski, P., Wang, J., Kuo, H.-C., Vomel, H., and Dirksen, R.: Evaluation of humidity correction methods for Vaisala RS92 tropical sounding data, *J. Atmos. Ocean. Tech.*, 32, 397–411, doi:10.1175/JTECH-D-14-00166.1, 2014.

Zhang, M. H. and Lin, J. L.: Constrained variational analysis of sounding data based on column-integrated budgets of mass, heat, moisture and momentum: approach and application to ARM measurements, *J. Atmos. Sci.*, 54, 1503–1524, 1997.

Zhang, M. H., Lin, J. L., Cederwall, R. T., Yiou, J. J., and Xie, S. C.: Objective analysis of ARM IOP data: method and sensitivity, *Mon. Weather Rev.*, 129, 295–311, 2001.

Zhao, C., Xie, S., Klein, S. A., McCoy, R., Comstock, J., Deng, M., Dunn, M., Hogan, R., Huang, D., Jensen, M. P., Mace, G. G., McFarlane, S., O'Connor, E., Protat, A., Shupe, M., Turner, D. D., and Wang, Z.: Understanding differences in current ARM ground-based cloud retrievals, *J. Geophys. Res.*, 117, D10206, doi:10.1029/2011JD016792, 2012.

Zhao, T., Dai, A., and Wang, J.: Trends in tropospheric humidity from 1970 to 2008 over China from a homogenized radiosonde dataset, *J. Climate*, 25, 4549–4567, doi:10.1175/JCLI-D-11-00557.1, 2012.

Comparison of Vaisala radiosondes RS41 and RS92

M. P. Jensen et al.

Table 5. Radiosonde launch characteristics.

Launch no.	Launch Time (LT = GMT – 5 h)	Maximum height (km)	Mean ascent rate (ms ⁻¹) to 200 hPa
1	3 Jun 12:55	31.096	4.8
2	3 Jun 15:43	29.881	5.6
3	3 Jun 17:46	28.660	4.7
4	3 Jun 22:07 (Night)	29.378	6.4
5	3 Jun 23:59 (Night)	30.334	6.0
6	4 Jun 12:57	29.487	6.2
7	4 Jun 14:50	29.954	6.0
8	4 Jun 17:13	29.808	6.2
9	5 Jun 09:50	28.088	6.1
10	5 Jun 11:34	28.119	5.9
11	5 Jun 14:57	28.729	5.5
12	5 Jun 21:59 (Night)	29.821	6.7
13	5 Jun 23:39 (Night)	29.800	5.6
14	6 Jun 15:26	28.078	6.3
15	6 Jun 19:16	28.799	6.3
16	7 Jun 09:35	28.725	6.0
17	7 Jun 11:16	28.449	6.0
18	7 Jun 20:09	29.697	5.1
19	7 Jun 22:08 (Night)	29.868	6.0
20	7 Jun 23:55 (Night)	25.957	6.1

Title Page

Abstract

Introduction

Conclusions

References

Tables

Figures

◀

▶

◀

▶

Back

Close

Full Screen / Esc

Printer-friendly Version

Interactive Discussion



Comparison of Vaisala radiosondes RS41 and RS92

M. P. Jensen et al.

Table 6. Surface observations of meteorological state for each launch. Pressure, temperature, relative humidity, wind speed and wind direction observations are from THWAPS (Temperature, Humidity, Wind and Pressure Sensor, www.arm.gov/instruments/thwaps). Sky cover from total sky imager and precipitable water vapor from microwave radiometer.

Flight no.	Pressure (hPa)	Temperature (°C)	RH (%)	Wind speed (ms ⁻¹)	Wind dir. (deg)	Sky cover (%)	Precipitable water vapor (cm)
1	975.95	31.0	60	9.0	173	54.28	3.57
2	973.83	31.8	51	8.5	166	22.54	3.32
3	971.74	31.1	51	10.5	173	10.64	3.24
4	969.07	26.0	70	4.6	174	–	2.76
5	970.07	25.9	65	7.2	191	–	2.85
6	970.12	32.4	46	4.1	223	23.74	3.84
7	969.75	33.1	46	4.0	205	71.99	3.90
8	969.10	32.9	49	4.0	180	99.55	4.17
9	968.44	22.0	96	4.0	74	99.78	4.44
10	968.31	21.7	86	5.5	76	99.65	4.07
11	970.96	28.6	63	3.8	127	1.67	3.68
12	973.60	26.3	81	2.8	59	–	4.56
13	973.40	23.9	88	9.5	79	–	4.77
14	975.02	28.9	56	1.8	295	35.26	3.74
15	972.55	26.6	76	5.0	95	91.53	3.74
16	975.50	20.9	78	7.4	325	17.69	2.94
17	975.58	24.0	65	5.0	320	16.34	2.97
18	976.12	25.1	64	1.6	10	47.64	3.37
19	976.38	22.6	73	3.8	58	–	3.31
20	977.46	20.4	84	1.3	62	–	3.23

Title Page

Abstract

Introduction

Conclusions

References

Tables

Figures



Back

Close

Full Screen / Esc

Printer-friendly Version

Interactive Discussion



Comparison of Vaisala radiosondes RS41 and RS92

M. P. Jensen et al.



Figure 1. Picture of two radiosonde types: RS92-SGP (left) and RS41-SG (right).

[Title Page](#)[Abstract](#)[Introduction](#)[Conclusions](#)[References](#)[Tables](#)[Figures](#)[Back](#)[Close](#)[Full Screen / Esc](#)[Printer-friendly Version](#)[Interactive Discussion](#)

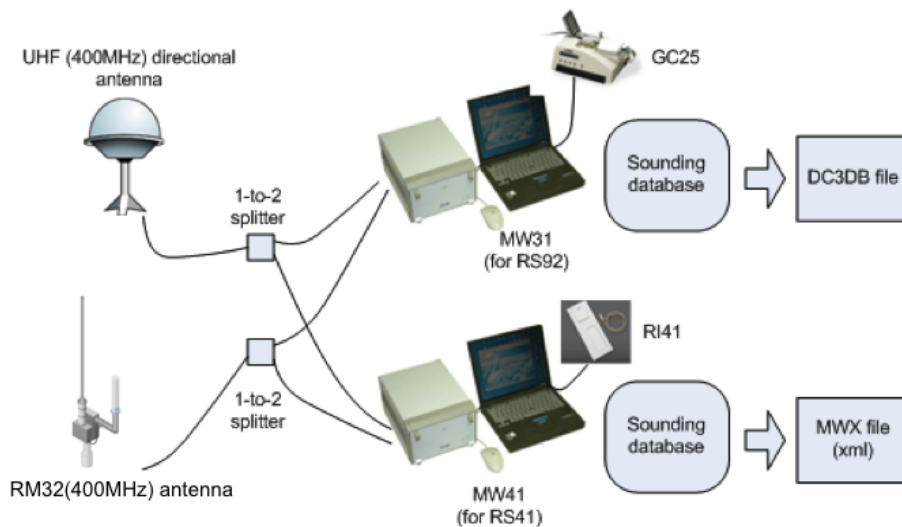


Figure 2. Experimental system set-up: Antennae, Sounding System and Ground Check System.

Comparison of Vaisala radiosondes RS41 and RS92

M. P. Jensen et al.

Title Page	
Abstract	Introduction
Conclusions	References
Tables	Figures
◀	▶
◀	▶
Back	Close
Full Screen / Esc	
Printer-friendly Version	
Interactive Discussion	



Comparison of Vaisala radiosondes RS41 and RS92

M. P. Jensen et al.

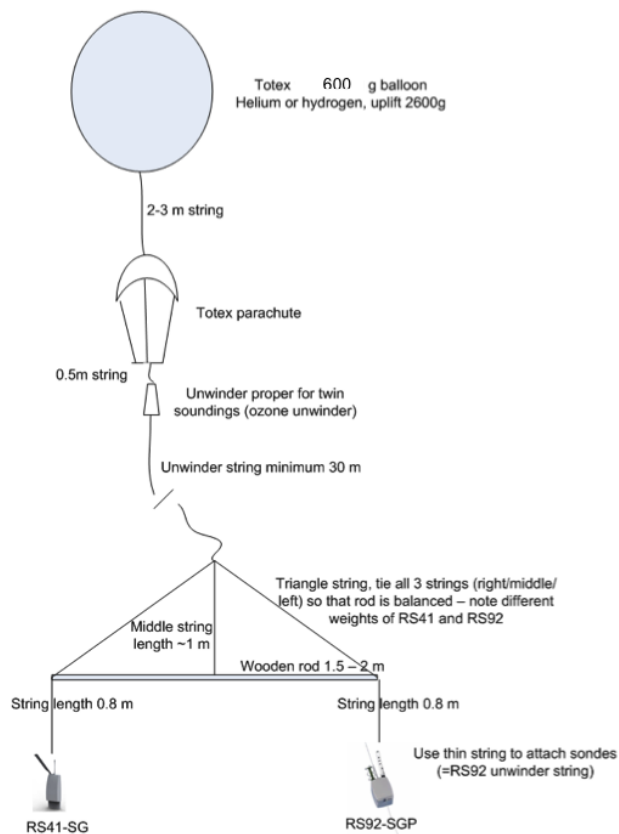


Figure 3. Experimental set-up: Balloon, Parachute, Unwinder, Rigging and Radiosondes.

Title Page

Abstract

Introduction

Conclusions

References

Tables

Figures

◀

▶

◀

▶

Back

Close

Full Screen / Esc

Printer-friendly Version

Interactive Discussion





Figure 4. Radiosonde Launch at the ARM Southern Great Plains site.

AMTD

8, 11323–11368, 2015

Comparison of Vaisala radiosondes RS41 and RS92

M. P. Jensen et al.

Title Page

Abstract

Introduction

Conclusions

References

Tables

Figures

◀

▶

◀

▶

Back

Close

Full Screen / Esc

Printer-friendly Version

Interactive Discussion



Comparison of Vaisala radiosondes RS41 and RS92

M. P. Jensen et al.

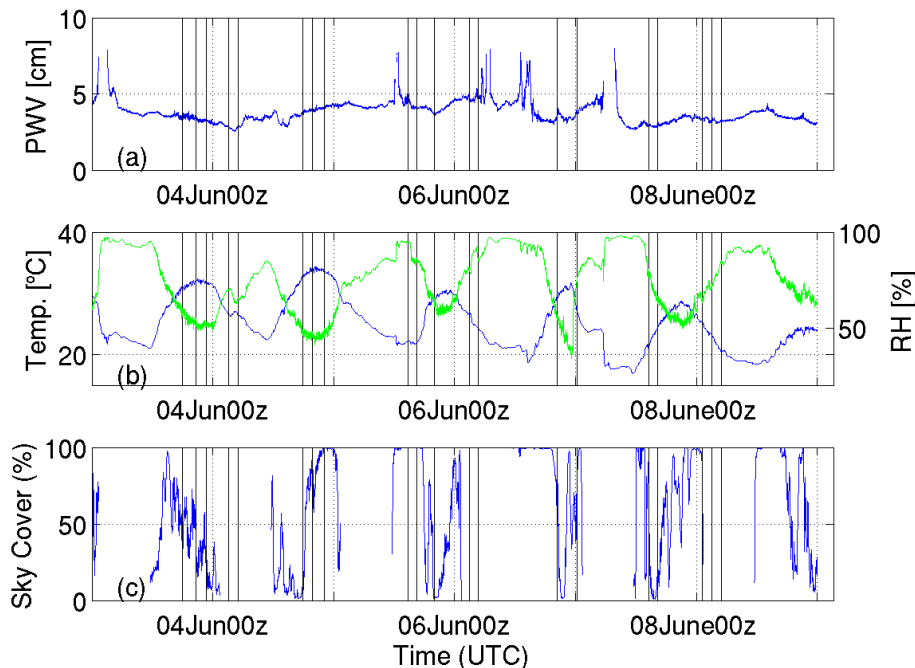


Figure 5. Time series of surface-based meteorological observations **(a)** precipitable water vapor (PWV) retrieved from a 2-channel microwave radiometer, **(b)** surface temperature (blue) and relative humidity (green), **(c)** hemispheric sky cover as observed by a total sky imager (TSI). Vertical black lines represent the times of radiosonde launches.

[Title Page](#)[Abstract](#)[Introduction](#)[Conclusions](#)[References](#)[Tables](#)[Figures](#)[◀](#)[▶](#)[◀](#)[▶](#)[Back](#)[Close](#)[Full Screen / Esc](#)[Printer-friendly Version](#)[Interactive Discussion](#)

Comparison of Vaisala radiosondes RS41 and RS92

M. P. Jensen et al.

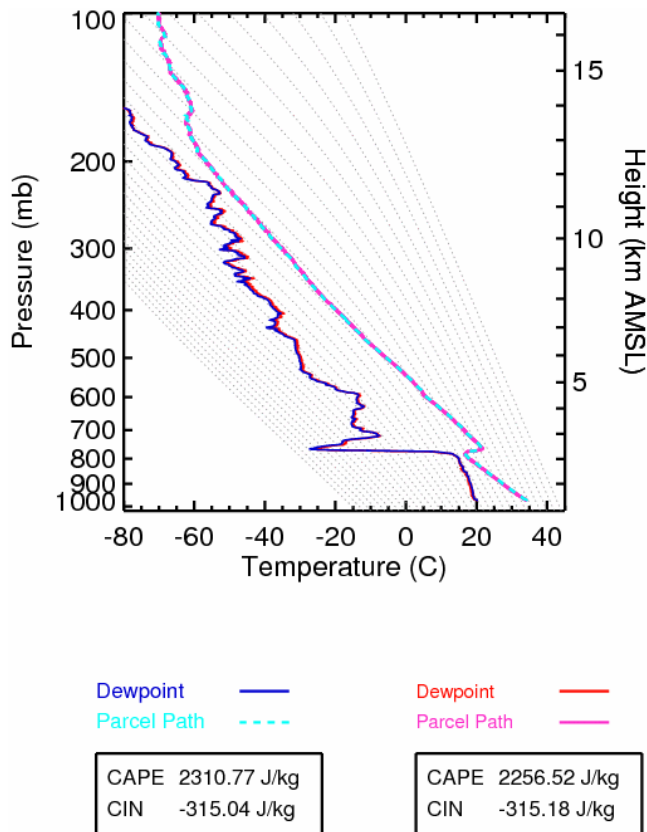


Figure 7. Skew-T plot from balloon flight #3 which was launched on 3 June 2014 at 17:46 LT. Dry bulb temperature for RS92 (cyan) and RS41 (magenta). Dew point temperature for RS92 (blue) and RS41 (red).

Title Page	
Abstract	Introduction
Conclusions	References
Tables	Figures
◀	▶
◀	▶
Back	Close
Full Screen / Esc	
Printer-friendly Version	
Interactive Discussion	



Comparison of
Vaisala radiosondes
RS41 and RS92

M. P. Jensen et al.

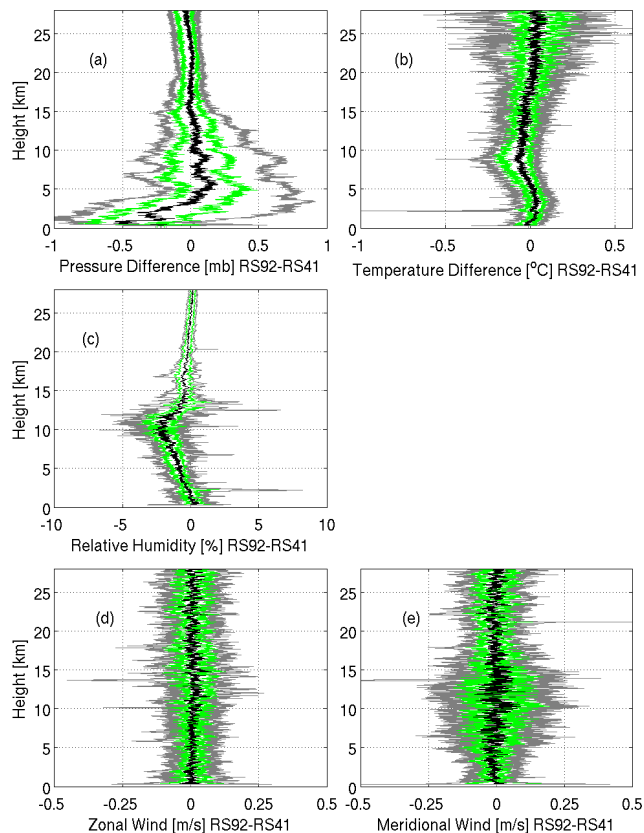


Figure 8. Vertical profiles of the median (black), 25th/75th percentile (green) and 10th/90th percentile (grey) differences between RS92 and RS41 observations (RS92-RS41) for **(a)** pressure, **(b)** dry bulb temperature, **(c)** relative humidity, **(d)** zonal wind and **(e)** meridional wind.

[Title Page](#)[Abstract](#)[Introduction](#)[Conclusions](#)[References](#)[Tables](#)[Figures](#)[◀](#)[▶](#)[◀](#)[▶](#)[Back](#)[Close](#)[Full Screen / Esc](#)[Printer-friendly Version](#)[Interactive Discussion](#)

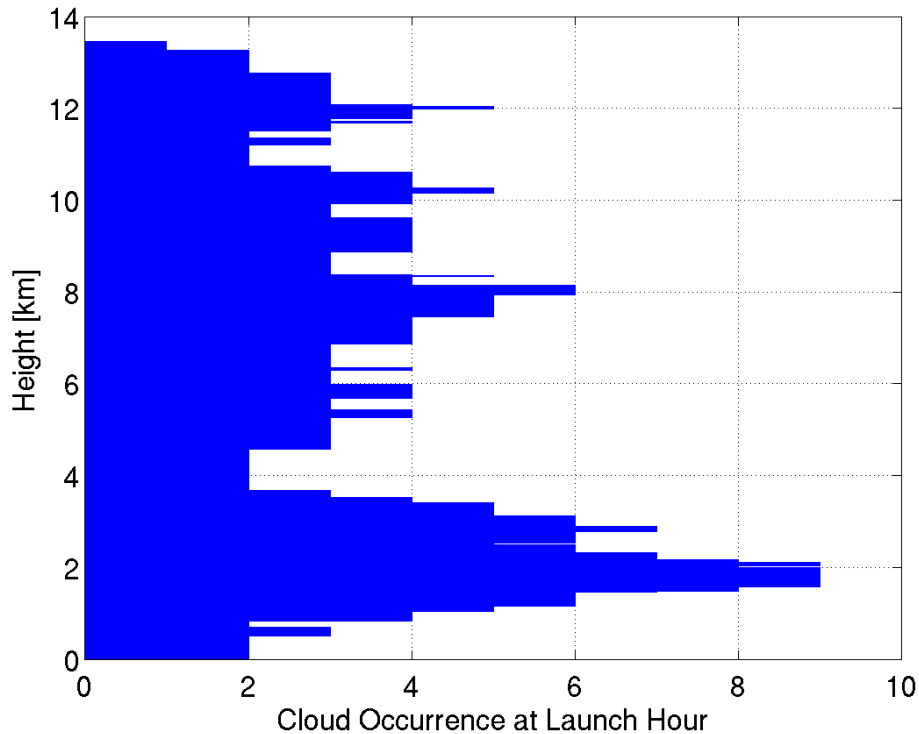


Figure 11. Summary of cloud occurrence at radiosonde launch times. Each bar represents the number of soundings for which the ARSCL product showed cloud occurrence greater than 25% for the hour of the launch for each height.

Comparison of Vaisala radiosondes RS41 and RS92

M. P. Jensen et al.

Title Page

Abstract Introduction

Conclusions References

Tables Figures

◀ ▶

◀ ▶

Back Close

Full Screen / Esc

Printer-friendly Version

Interactive Discussion



Comparison of Vaisala radiosondes RS41 and RS92

M. P. Jensen et al.

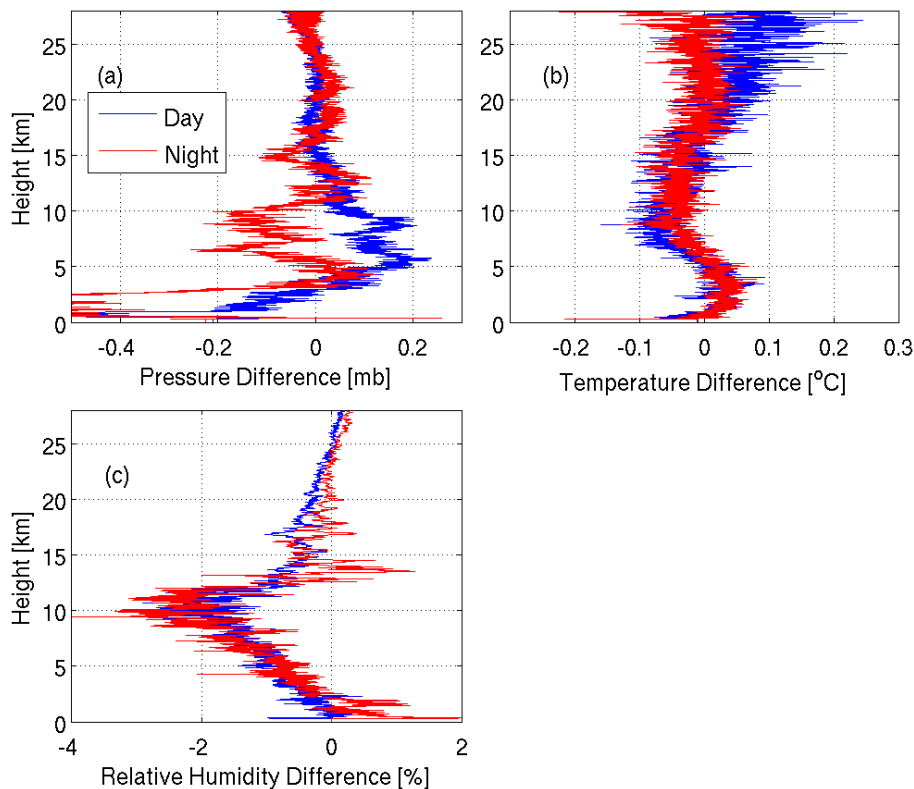


Figure 13. Differences between RS92 and RS41 radiosondes (RS92-RS41) for daytime (blue) and nighttime (red) flights for **(a)** pressure, **(b)** temperature and **(c)** relative humidity.

Title Page

Abstract

Introduction

Conclusions

References

Tables

Figures

◀

▶

◀

▶

Back

Close

Full Screen / Esc

Printer-friendly Version

Interactive Discussion



**Comparison of
Vaisala radiosondes
RS41 and RS92**

M. P. Jensen et al.

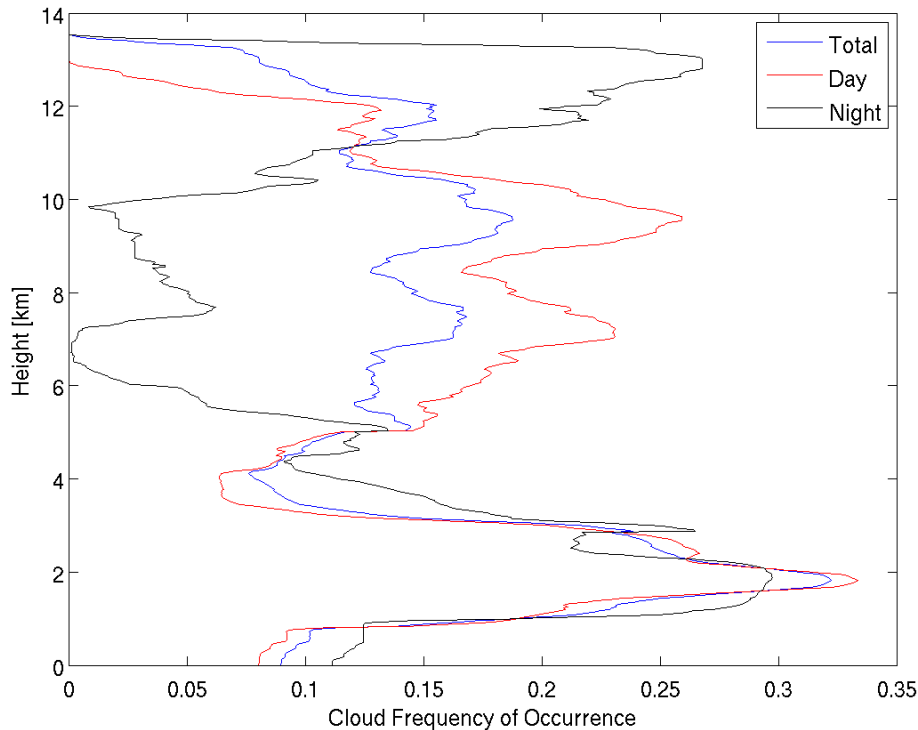


Figure 14. Comparison of cloud frequency of occurrence for daytime, nighttime and all sounding launch times. Cloud frequency of occurrence is calculated using the ARSCL product and compiled over a 1 h window following each sonde launch time.

[Title Page](#)[Abstract](#)[Introduction](#)[Conclusions](#)[References](#)[Tables](#)[Figures](#)[◀](#)[▶](#)[◀](#)[▶](#)[Back](#)[Close](#)[Full Screen / Esc](#)[Printer-friendly Version](#)[Interactive Discussion](#)

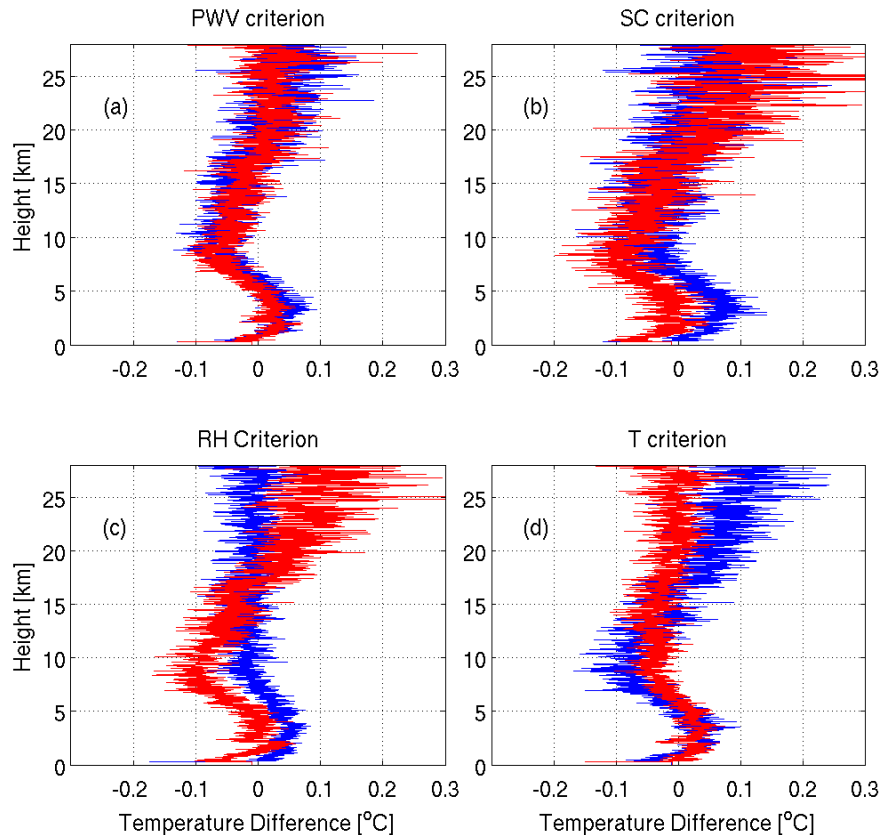
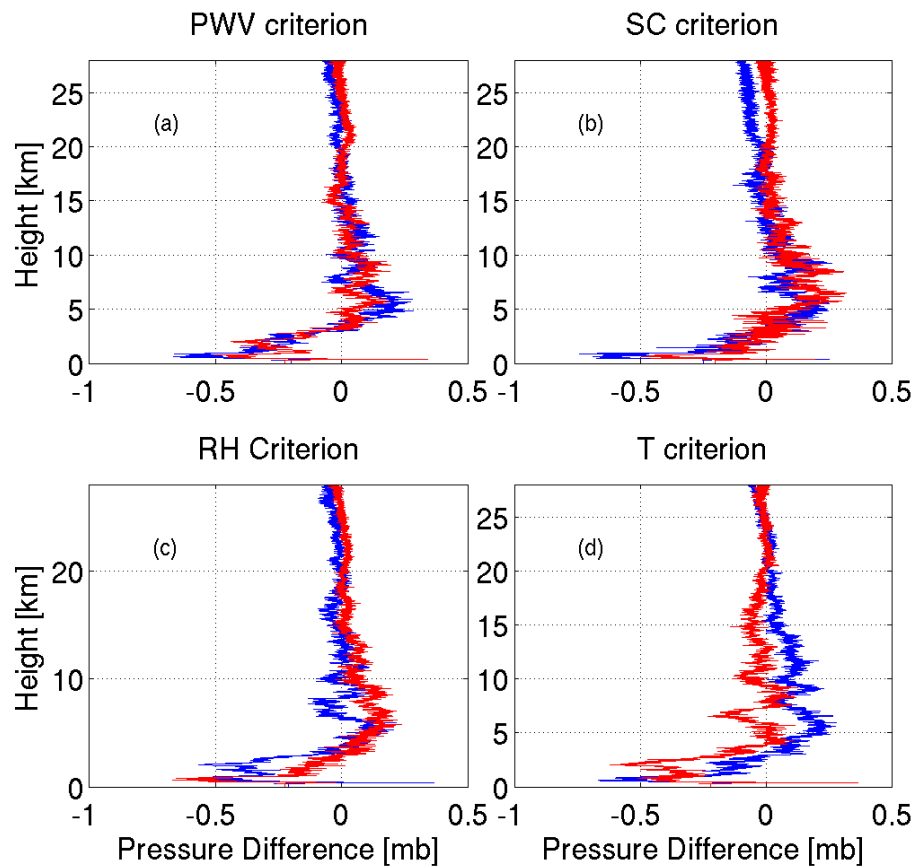


Figure 15. Temperature difference between RS92 and RS41 radiosondes (RS92-RS41) as a function of height for sonde launches with **(a)** PWV > 3.6 cm (blue) and those with PWV < 3.6 cm (red), **(b)** SC > 40% (blue) and SC < 40% (red), **(c)** surface RH > 65.2% (blue) and surface RH < 65.2% (red), and **(d)** surface temperature > 26.5°C and surface temperature < 26.5°C (red). The PWV/SC/RH/T = 3.6 cm/40%/65.2%/26.5°C are based on the median values for the 20 balloon launches during the intercomparison.

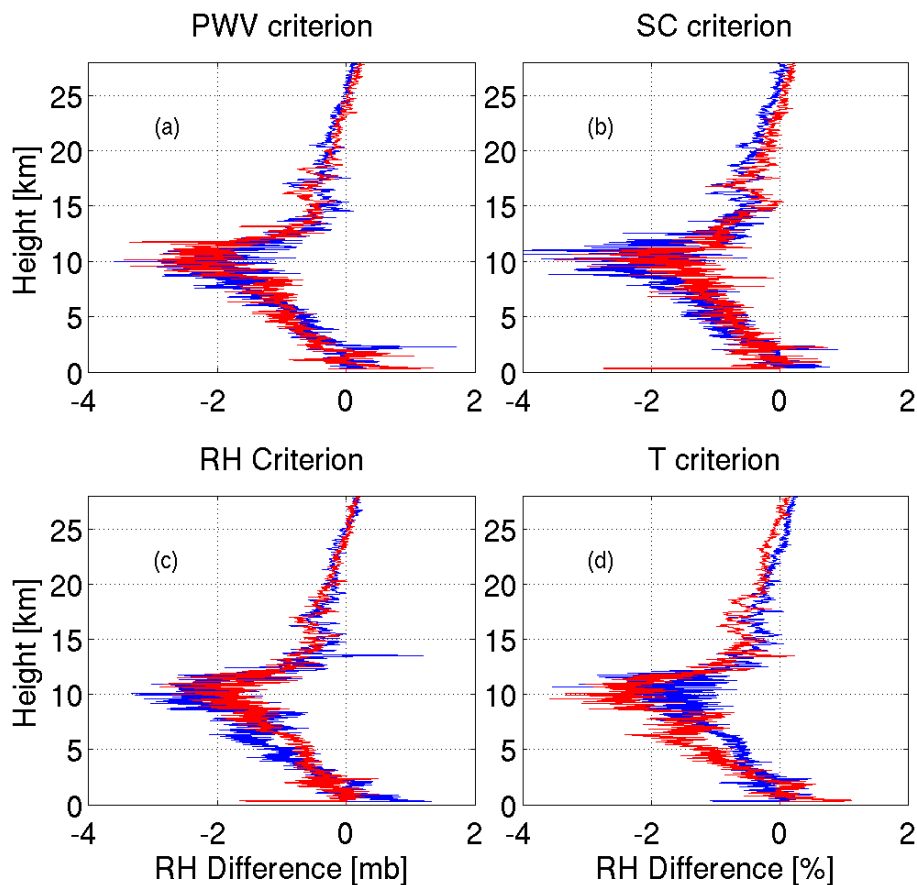
**Comparison of
Vaisala radiosondes
RS41 and RS92**

M. P. Jensen et al.

**Figure 16.** Same as Fig. 15 for pressure differences.[Title Page](#)[Abstract](#)[Introduction](#)[Conclusions](#)[References](#)[Tables](#)[Figures](#)[◀](#)[▶](#)[◀](#)[▶](#)[Back](#)[Close](#)[Full Screen / Esc](#)[Printer-friendly Version](#)[Interactive Discussion](#)

**Comparison of
Vaisala radiosondes
RS41 and RS92**

M. P. Jensen et al.

**Figure 17.** Same as Fig. 15 for relative humidity differences.

Comparison of Vaisala radiosondes RS41 and RS92

M. P. Jensen et al.

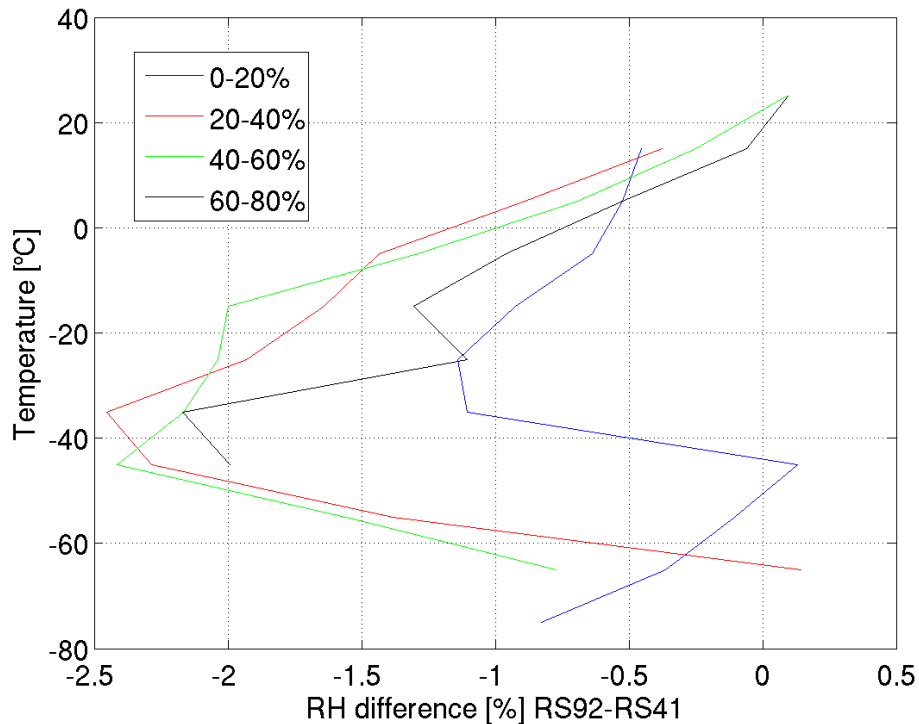


Figure 18. Difference in relative humidity between the RS92 and RS41 radiosondes as a function of temperature for four different relative humidity ranges.

[Title Page](#)[Abstract](#)[Introduction](#)[Conclusions](#)[References](#)[Tables](#)[Figures](#)[◀](#)[▶](#)[◀](#)[▶](#)[Back](#)[Close](#)[Full Screen / Esc](#)[Printer-friendly Version](#)[Interactive Discussion](#)

Comparison of Vaisala radiosondes RS41 and RS92

M. P. Jensen et al.

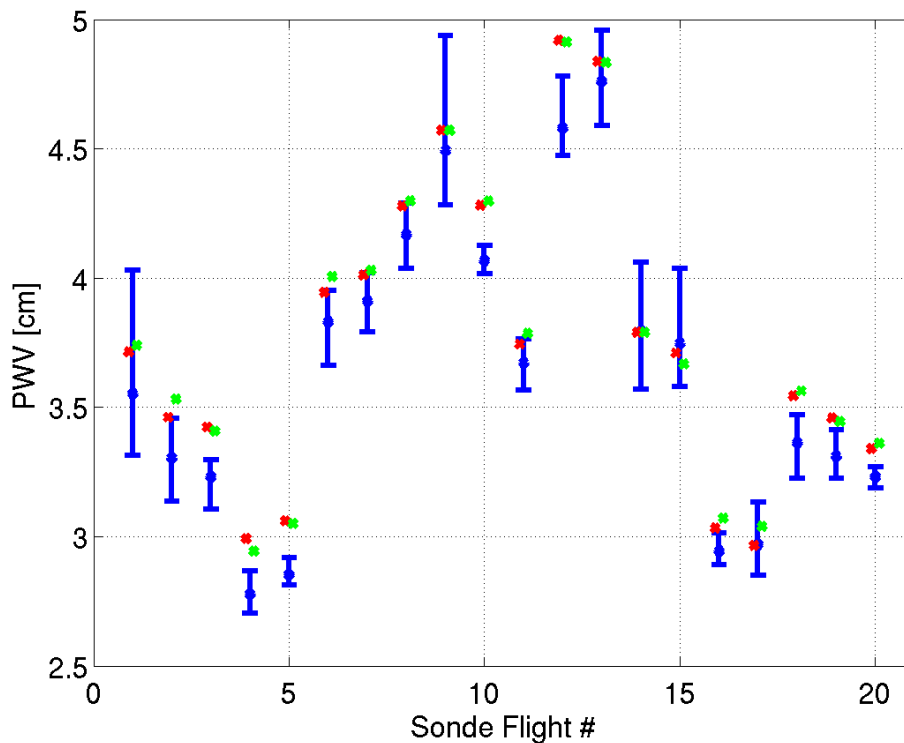


Figure 19. Comparison of precipitable water vapor for the RS92 (red), RS41 (green) and microwave radiometer (blue). Error bars on the MWR observations represent the range of observed PWV during the first half hour of each balloon launch.